Send Orders for Reprints to reprints@benthamscience.ae

Medicinal Chemistry, **2016**, *12*, **63-73**

Pharmacophore-Based Virtual Screening for Identification of Novel Neuraminidase Inhibitors and Verification of Inhibitory Activity by Molecular Docking

Sidra Batool[1], Gohar Mushtaq[2], Warda Kamal[3] and Mohammad A. Kamal[4]*

[1]Department of Biosciences, Comsats Institute of Information Technology, Islamabad, Pakistan; [2]Department of Biochemistry, College of Science, King Abdulaziz University, Jeddah 21589, Saudi Arabia; [3]Biomediotronics, Enzymoic, 7 Peterlee Pl, Hebersham, NSW 2770, Australia; [4]Metabolomics & Enzymology Unit, Fundamental and Applied Biology Group, King Fahd Medical Research Center, King Abdulaziz University, P. O. Box 80216, Jeddah 21589, Saudi Arabia

Mohammad A. Kamal

Abstract: Oseltamivir and Zanamivir are two of the recently licensed neuraminidase inhibitors used for the treatment of influenza. However, alternative antiviral agents are needed due to the development of resistant mutations in Oseltamivir subtype H1N1 and H5N1 avian influenza A viruses, the latter being a highly pathogenic avian virus that can be transferred to humans upon immediate contact with H5N1 infected poultry or surface. Novel drug inhibiting group 1 neuraminidases may potentially be developed through addition of extra substituent moieties to existing inhibitor skeletons. Another approach involves virtual screening of existing inhibitor skeletons which we have reported using novel ligands of H5N1 via virtual screening approach. In this study, we have used 3D structure of avian influenza virus H5N1 neuraminidase as target against a ligand dataset of four known neuraminidase inhibitors for *in silico* analysis. Using the dataset of known four inhibitors, a pharmacophore model was developed using ligand-based pharmacophore modeling strategy. This pharmacophore model was then used for virtual screening of natural compounds library taken from Princeton database. New hits that shared features of our pharmacophore model and binding interactions with receptor residues have been reported in this study. As more antiviral agents are required, the reported hits in our study may play an important role as novel antiviral agents against influenza virus.

Keywords: Neuraminidase inhibitors, virtual screening, pharmacophore model, antiviral agents.

INTRODUCTION

Influenza is a highly contagious virus that causes varying degrees of symptoms ranging from mild flu-like symptoms to severe respiratory illness and death. Out of the three types of influenza virus (A, B and C), type A infects a wide range of avian as well as mammalian species. This virus contains glycoproteins, haemagglutinin and neuraminidase in its membranes which play crucial roles in the Influenza infection. Haemagglutinin is an antigenic glycoprotein that acts as a mediator between cell-surface sialic acid receptor binding to initiate the viral infection. Cellular glycoproteins and sialic acid are then removed from viral cells by neuraminidase to enable its release which spreads infection to new cells [1]. Type A influenza virus is divided into two subcategories according to the antigenic properties of haemagglutinin and neuraminidase molecules: Haaemagglutinin (H1–H16) contains 16 sub-groups of the virus ranging from H1 to H16 whilst the later contains a smaller range (N1–N9) [2]. The three pandemics that occurred in the twentieth century and wiped out a portion of human population were caused by virus containing various combinations of haemagglutinin and neurminidase sub-types: H1N1 in 1918, H2N2 in 1957 and H3N2 in 1968. In 1997, H5N1 avian influenza virus caused a pandemic in Hong Kong human population, with virus originating from the live poultry chicken market [3,4].

Neuraminidases N1 and N2 are another subtype of influenza virus which are known to affect the human population [5]. They belong to two phylogenetic categories with the first group containing subtypes N1, N4, N5 and N8 subtypes and the second group containing N2, N3, N6, N7 and N9. All catalytic sites of neuraminidase influenza hold the following three arginine residues, Arg 118, Arg 292 and Arg 371, which bind carboxylate of the substrate, sialic acid. On the other hand, Arg 152 and Glu 276 have interactions with acetamido 9 substituent of the substrate and with 8- and 9-hydroxyl groups of the substrate to form hydrogen bonds, respectively [6,7].

Nuraminidase, a proven anti-influenza drug target, holds great promise for further research in the development of new virus inhibitors, particularly due to the emergence of resistant virus strains to current dugs as a result of genetic mutations [8-11]. Such antiviral drugs work through mechanisms

*Address correspondence to this author at the Metabolomics & Enzymology Unit, Fundamental and Applied Biology Group, King Fahd Medical Research Center, King Abdulaziz University, P. O. Box 80216, Jeddah 21589, Saudi Arabia; E-mail: prof.makamal@lycos.com

1875-6638/16 $58.00+.00

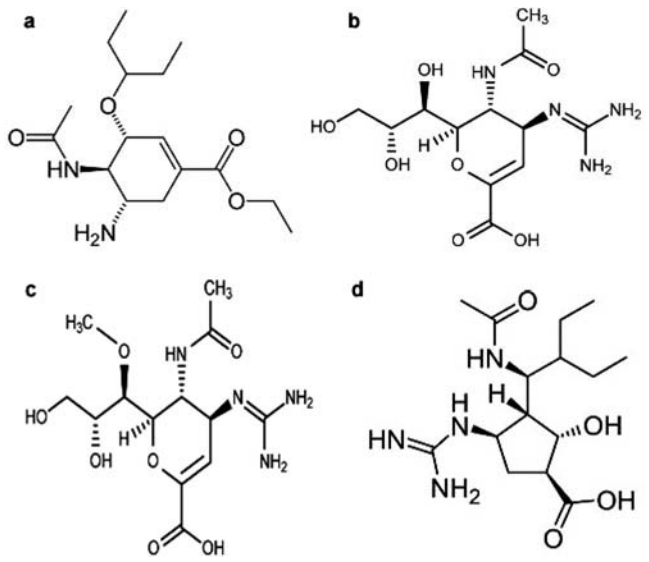

Fig. (1). 2D structures of ligand data set based on neuraminidase inhibitors (a) Oseltamivir, (b) Zanamivir, (c) Laninamivir, and (d) Peramivir.

which inhibit function of the viral neuraminidase protein, thus preventing the virus from integrating with other cells, resulting in no reproduction and spread of virus to healthy cell bodies. A number of *in silico* studies have been reported that have investigated various computational approaches targeting H5N1 influenza A virus [12-15]. During the past few years, significant progress in studying influenza A virus, both experimentally [16-19] and theoretically [20-29], has been reported. There are various types of neuraminidase inhibitors which act against both influenza A and influenza B. The knowledge of protein 3D (three-dimensional) structures or their complexes with ligands is crucial for rational drug design. Although X-ray crystallography is a powerful tool in determining these structures, it is time-consuming and expensive, and, most importantly, not all proteins can be successfully crystallized. Membrane proteins are difficult to crystallize and most of them will not dissolve in normal solvents. Therefore, X-ray structures of very few membrane protein structures have been determined so far. NMR is indeed a very powerful tool in determining the 3D structures of membrane proteins (see, *e.g.*, [30-33]), but it is also time-consuming and costly. In order to acquire structural information in a timely manner, a series of 3D protein structures were developed by means of structural bioinformatics tools (for comprehensive review see references [34-38]) and were found very useful for stimulating drug development. In view of this, the computational (or *in silico*) methods were also utilized in this study for screening, identifying and verifying novel neuraminidase inhibitors. For the purpose of this study against H5N1 virus, the following ligand dataset is used: Oseltamivir (Tamiflu), Zanamivir (Relenza), Laninamivir (Inavir), and Peramivir [39]. A pharmacophore model was developed using this ligand dataset of known inhibitors. To identify novel ligands on the basis of our developed pharmacophore model, we have performed virtual screening of a library that contains 50,000 natural compounds taken from the Princeton Database (*www.princetonbio.com*). New hits that showed exact pharmacophore features and binding interactions with receptor protein are reported here.

Table 1. List of grid and docking parameters used to perform docking experiment.

Grid Parameters		**Docking Parameters**	
Spacing	0.375 Å	Energy evaluations	2.5×10^6
Grid Center	80X Å	Iterations	27000
	80Y Å	Mutation rate	0.02
	80Z Å	Crossover rate	0.80
		Elitism value	1
		RMS Tolerance	1.0 Å

METHODS

As the structure of H5N1 neuraminidase virus contains potential of new opportunities for drug design, 3D structure of H5N1 (PDB id: 2HTQ) was used as a receptor. The binding residues for this structure include Arg118, Asp151, Arg152, Trp178, Glu276, Tyr347, and Arg371 [40]. The information of the binding pocket of a receptor for its ligand is very important for drug design, particularly for conducting mutagenesis studies [38]. In the literature, the binding pocket of a protein receptor to a ligand is usually defined by those residues that have at least one heavy atom (i.e., an atom other than hydrogen) within a distance of 5Å from a heavy atom of the ligand. This same criterion was originally used to define the binding pocket of ATP in the Cdk5-Nck5a* complex [41] that later proved quite useful in identifying functional domains and stimulating the relevant truncation experiments [42]. Similar approach has also been used to define the binding pockets of many other receptor-ligand interactions important for drug design [43-47]. Four experimentally known neuraminidase inhibitors, i.e. Oseltamivir, Zanamivir, Laninamivir, and Peramivir were taken as ligands. (Fig. **1**) shows 2D structure of these inhibitors.

Docking of neuraminidase inhibitors was performed using Autodock 4.2 software [48]. To determine suitable binding orientations and conformations of neuraminidase inhibitors with H5N1 protein according to specified instructions, automated dockings were carried out. Each docking experiment consisted of 100 runs, yielding 100 docked conformations. Briefly, receptor proteins were designated to polar hydrogen atoms and Kollman charges, whilst the ligands were assigned Gasteiger partial charges. All non-polar hydrogen atoms were combined and torsions for ligands were enabled to rotate during docking procedure. To generate grid maps, AutoGrid software was used which allowed the placement of each grid in the center of corresponding receptor. The following strategies were used for all ligands: random starting positions, random orientations, and torsions. The translation, quaternion and torsion strategies were adopted from default values programmed in the AutoDock. Lamarckian genetic algorithm was considered for minimization via default generics. The parameters for the docking experiments are shown in Table **1**.

Table 2. Energy values for docking experiment of four neuraminidase inhibitors with H5N1 strain.

Properties	Ligands			
	Oseltamivir	**Zanamivir**	**Laninamivir**	**Peramivir**
Binding Energy (kcal/mol)	-6.01	-6.92	-6.87	-4.75
Ki (μM)	39.55	8.43	9.22	331.02
Intermolecular Energy (kcal/mol)	-8.69	-9.91	-9.85	-7.43
vdW + Hbond + desolv Energy (kcal/mol)	-6.43	-7.4	-7.4	-5.1
Electrostatic Energy (kcal/mol)	-2.26	-2.51	-2.45	-2.33
Final Total Internal Energy (kcal/mol)	-0.99	-2.21	-2.26	-0.42
Torsional Free Energy (kcal/mol)	2.26	2.98	2.98	2.68
Unbound System's Energy (kcal/mol)	-0.99	-2.21	-2.26	-0.42
Temperature(K)	298.5	298.5	298.5	298.5

Many remarkable biological functions in proteins and DNA and their profound dynamic mechanisms, such as switch between active and inactive states [49,50], cooperative effects [51], allosteric transition [46] and intercalation of drugs into DNA [52], can be revealed by studying their internal motions as summarized in one comprehensive review [53]. Likewise, to really understand the interaction of a protein receptor with its ligand and to reveal its binding mechanism, we should consider not only the concerned static structures but also the dynamic information obtained by simulating their internal motions or dynamic processes, and efforts will be made in this regards in our future work. Keeping in mind the objective of this study, the type of docking performed was rigid docking, as the receptor under study was studied in its static form rather than the dynamic form.

The geometry optimized conformations of four inhibitors were used as basic skeleton for ligand-based pharmacophore modeling. The ligand-based strategy derives pharmacophore models from a set of ligands in the absence of a macromolecule structure by considering the conformational flexibility parameter derived from known ligands. In this study, Ligand Scout tool [54] was used to develop three dimensional pharmacophore hypothesis using a set of four compounds (a-d). Ligand Scout generates structure-based as well as ligand-based pharmacophore models. The developed pharmacophore model was used for virtual screening of natural compounds library taken from the Princeton database for identifying novel inhibitors against avain influenza virus. Pharmacophore modeling and virtual screening approaches have been extensively used for identification of novel ligands [55-57].

RESULTS AND DISCUSSION

Binding Analysis of Neuraminidase Inhibitors Docked to Neuraminidase

As this study is based on computational predictions, we have used binding information of the receptor against neuraminidase inhibitors for validation of our results. The energy values of docking experiments lie in favorable range. Table **2** shows the binding, intermolecular, vdW + Hbond + desolv, electrostatic, final internal energy, torsional energy and system's unbound energies along with inhibition constant values.

Table **2** shows that the four ligands showed favorable energy values of binding from docking experiments. While comparing the docking results of these inhibitors, we observed that Zanamivir and Laninamivir have the lowest binding energy and predicted inhibition constant values. On the basis of lower binding free energy, and better electrostatic interaction and inhibition constant values of these neuraminidase inhibitors against H5N1, we found out that Zanamivir and Laninamivir would be more potent inhibitors for H5N1 inhibition than Oseltamivir and Peramivir. Also, the interaction data supported this statement as Zanamivir and Laninamivir showed maximum number of hydrogen bonds with receptor binding site as compared to Oseltamivir and Peramivir (Table **3**). (Fig. **2**) also clearly shows that the docked complexes of four inhibitors exhibited binding with critical residues of the receptor protein H5N1.

A comparative overview of interactions of binding residues of receptor protein with the inhibitors is also represented in Table **3**. Among the binding residues, those involved in making hydrogen bonds with the inhibitors are shown with the type of hydrogen bond formed (in the context of hydrogen bond donor and acceptor) and distance between the atoms forming them.

Evaluation of Pharmacophore Model and Analysis

The ligand-based pharmacophore model was developed using ligand-based pharmacophore modeling from the ligand dataset of Oseltamivir, Zanamivir, Laninamivir and Peramivir. Two dimensional pharmacophore model for each ligand is shown in (Fig. **3**). Green arrows indicate the presence of hydrogen bond donors (HBD) while the red arrows represent hydrogen bond acceptors (HBA). Blue color displays positive ionizable areas.

The pharmacophoric features for each inhibitor are shown in Table **4**.

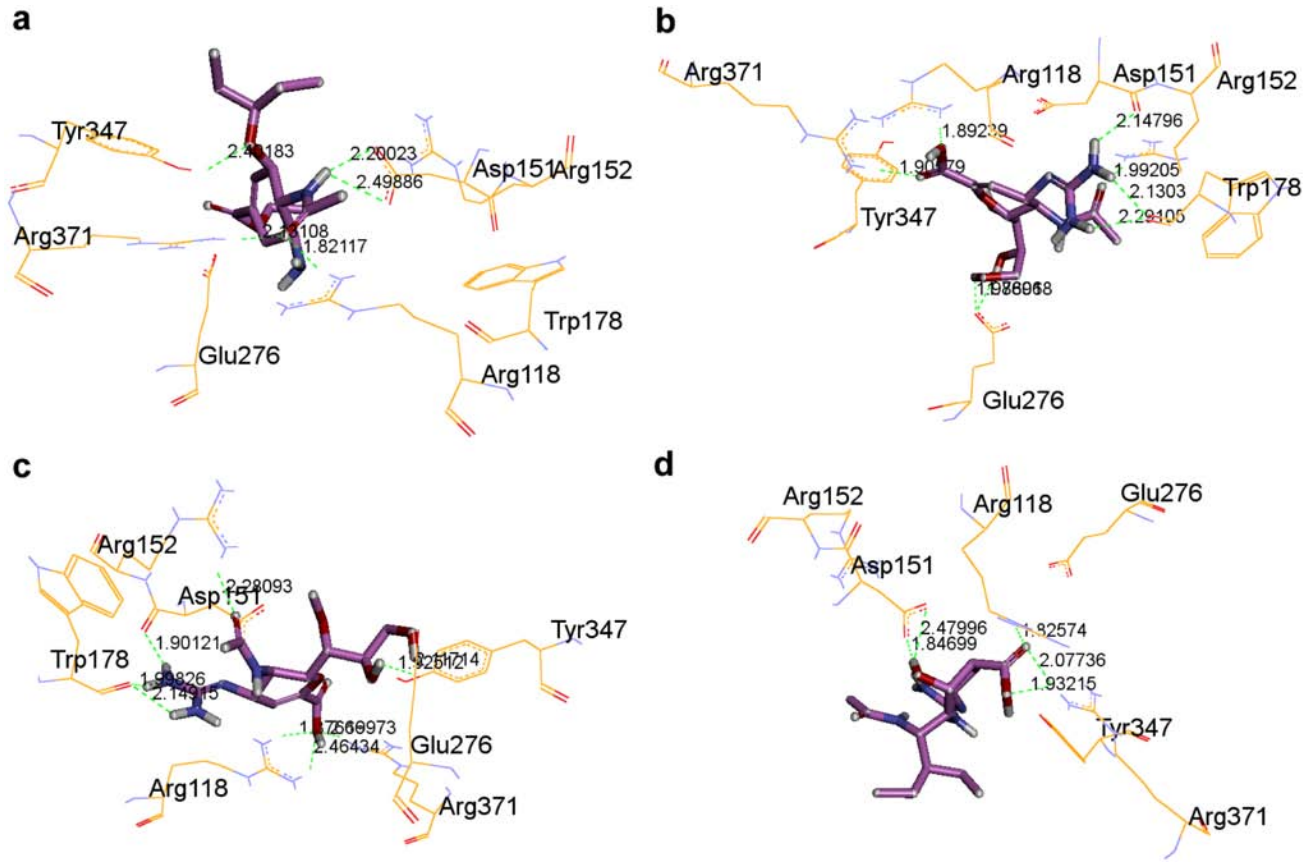

Fig. (2). Docking interactions of neuraminidase with different inhibitors: (a) Oseltamivir, (b) Zanamivir, (c) Laninamivir, and (d) Peramivir. Residues and hydrogen bond distances (Å) are labeled, hydrogen bonds are represented by Green dotted lines. Coloring scheme is according to atom type: Hydrogen, Grey; Nitrogen, Blue; Oxygen, Red; inhibitor's Carbon, Purple; protein's Carbon, Orange. (For interpretation of the references to color in this figure legend, the reader is referred to the web version of this paper).

Table 3. Detailed interactions of residues involved in binding interactions during docking with the inhibitor data set. HDP represents involvement in a hydrophobic interaction, while Å represents the distance, in angstrom units, among atoms (neuraminidase residue atom-inhibitor atom) involved in forming the hydrogen bonds.

Inhibitors	Oseltamivir		Zanamivir		Laninamivir		Peramivir	
Residues	**Bond**	**Å**	**Bond**	**Å**	**Bond**	**Å**	**Bond**	**Å**
Arg118	NH-O	1.82	NH-O	1.89	NH-O	1.88	NH-O	1.83
					NH-O	2.46		
Asp151	O-HN	2.20	O-HN	2.15	O-HN	1.90	O-HO	1.85
	O-HN	2.50					O-HO	2.48
Arg152	HDP		NH-O	1.99	NH-O	2.28	HDP	
Trp178	HDP		O-HN	2.13	O-HN	2.00	-	
			O-HN	2.29	O-HN	2.15		
Glu276	HDP		O-HO	1.86	O-HO	1.92	HDP	
			O-HO	1.98	O-HO	2.12		
Tyr347	OH-O	2.40	HDP		HDP		HDP	
Arg371	NH-O	2.13	NH-O	1.91	NH-O	2.20	NH-O	1.93
							NH-O	2.08

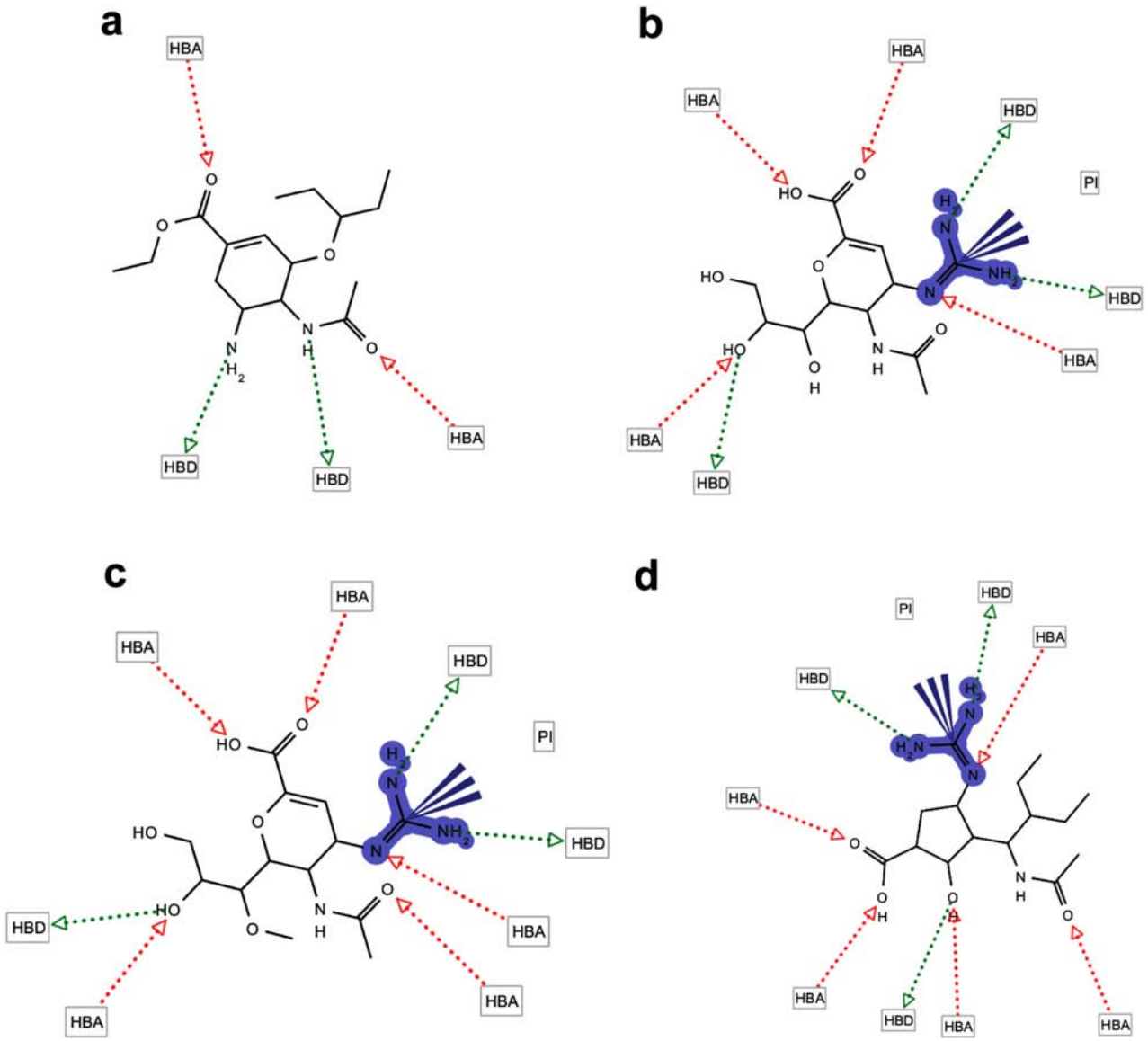

Fig. (3). 2D Depiction pharmacophore models: (a) Oseltamivir (b) Zanamivir (c) Laninamivir (d) Peramivir.

Table 4. Pharmacophoric features of selected inhibitors.

Ligand	HBA	HBD	PI
Oseltamivir	++	++	-
Zanamivir	++++	+++	+
Laninamivir	+++++	+++	+
Peramivir	+++++	+++	+

The common pharmacophore with shared features obtained by alignment of the four inhibitors is shown in (Fig. **4**). The common pharmacophore feature include one positive ionizable area, five hydrogen acceptors and three hydrogen donors.

For the common pharmacophore model, we have also calculated distances among features of pharmacophore. The suggested 3D pharmacophore model and distances between the common pharmacophoric characteristics of the proposed model are shown in (Fig. **5**).

We have used this pharmacophore model for virtual screening of a library taken from the Princeton Database. This library consists of 50,000 natural compounds. We wanted to identify and report those natural compounds that

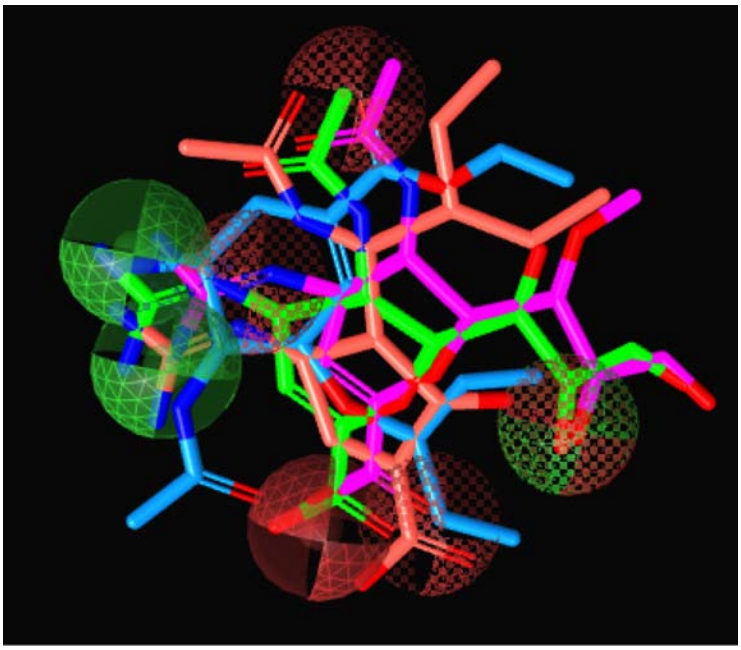

Fig. (4). Alignment of the four compounds with features of generated pharmacophore. Oseltamivir, Blue; Zanamivir, Green; Laninamivir, Purple; Peramivir, Orange. (For interpretation of the references to color in this figure legend, the reader is referred to the web version of this paper).

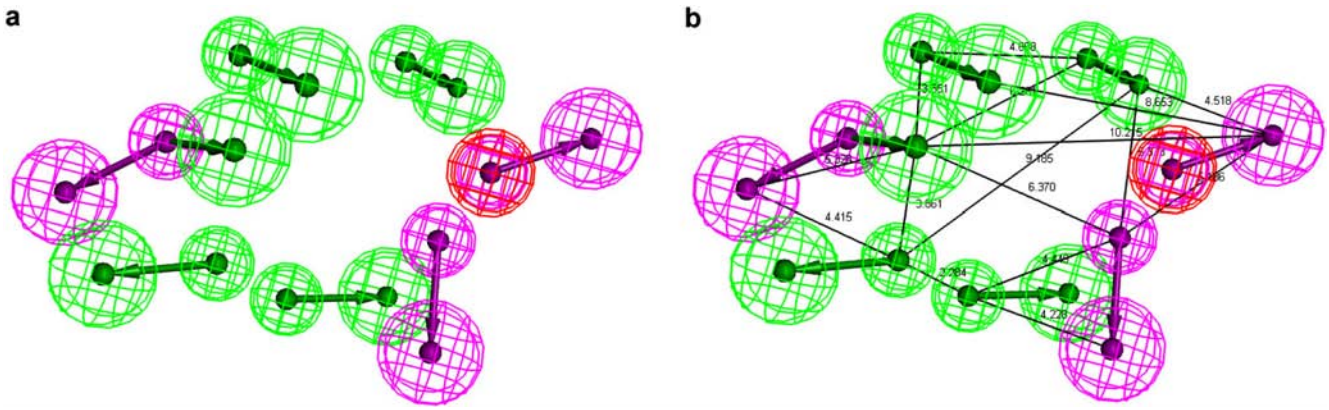

Fig. (5). (a) 3D Pharmacophore model of four compounds showing geometrical relationship among pharmacophore features. Positive ionizable area (PI) is represented by red meshed sphere, hydrogen bond donor (HBD) by a pair of magenta spheres, and hydrogen bond acceptor (HBA) by a pair of green spheres. The smaller sphere represents the location of the HBA atom on the ligand, while the larger one indicates the location of HBD atom on the receptor. (b) Distances (Å) among the centers of selected features are labeled. (For interpretation of the references to color in this figure legend, the reader is referred to the web version of this paper).

shared pharmacophore features of neuraminidase inhibitors along with interactions with critical binding residues of H5N1 receptor with favorable energy values.

Virtual Screening of Princeton Library

A library of natural compounds consisting of 50,000 compounds from Princeton Database was screened using the 3D pharmacophore model. Out of the screened compounds, 15,000 compounds that shared pharmacophore-like features were identified. The extracted compounds were further checked using various filters like Lipinski's rule. As a result, 300 compounds were extracted on the basis of exact pharmacophore features including three hydrophobic regions, two aromatic rings, one hydrogen acceptor and one hydrogen donor. These 300 compounds were subsequently used for docking analysis. Next, receptor and ligand complementarities were checked and 240 compounds were filtered on the basis of these criteria. Compounds having positive binding energies were eliminated leaving 180 compounds for further study. Dockings were done using Autodock 4.2 and analyzed carefully for these compounds with structure of H5N1 virus strain. Analysis revealed that out of 180 compounds, 12 compounds exhibited frequent hydrogen and hydrophobic interactions with the critical binding residues of the receptor. Two-dimensional structures of shortlisted 12 hits are indicated in (Fig. **6**).

Energy values as a result of docking experiments for these twelve hits with H5N1 receptor are shown in Table **5**.

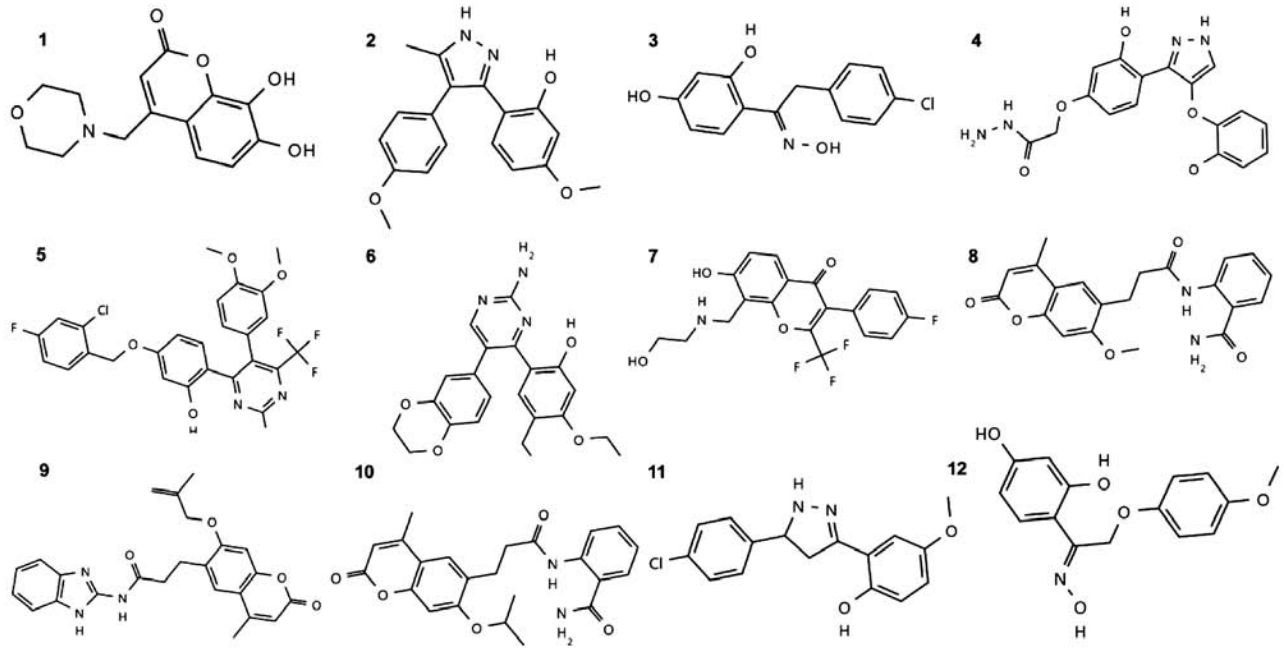

Fig. (6). 2D Representation of screened hit compounds from Princeton library.

Table 5. Energy values for the screened compounds from Princeton library with neuraminidase as receptor.

Properties/Ligand	1	2	3	4	5	6	7	8	9	10	11	12
Binding Energy (kcal/mol)	-6.26	-6.22	-6.29	-6.49	-5.94	-6.39	-5.71	-6.69	-7.22	-4.76	-6.55	-5.01
Ki (μM)	25.95	27.63	24.57	17.35	43.9	20.81	65.22	12.41	5.08	322.82	15.92	213.21
Intermolecular Energy (kcal/mol)	-7.45	-7.71	-8.38	-9.18	-8.39	-8.47	-8.1	-8.48	-9.31	-6.85	-7.74	-7.69
vdW + Hbond + desolv Energy (kcal/mol)	-5.89	-7.69	-8.28	-8.9	-8.51	-8.48	-7.87	-8.48	-9.22	-6.91	-7.64	-7.69
Electrostatic Energy (kcal/mol)	-1.56	-0.02	-0.09	-0.28	-0.42	0.01	-0.23	-0.01	-0.1	0.06	-0.1	0.0
Final Total Internal Energy (kcal/mol)	-0.55	-0.74	-0.17	-1.31	-0.96	-0.33	-0.54	-0.5	-0.78	-0.83	-0.72	-0.47
Torsional Free Energy (kcal/mol)	1.19	1.49	2.09	2.68	2.98	2.09	2.39	1.79	2.09	2.09	1.19	2.68
Unbound System's Energy (kcal/mol)	-0.55	-0.74	-0.17	-1.31	-0.96	-0.33	-0.54	-0.5	-0.78	-0.83	-0.72	-0.47
Temperature(K)	298.5	298.5	298.5	298.5	298.5	298.5	298.5	298.5	298.5	298.5	298.5	298.5

Binding energy values range from -4.76 Kcal/mol to -7.22 Kcal/mol. Intermolecular energy values range from -7.45 Kcal/mol to -9.31 Kcal/mol. Compound 9 showed the lowest value of energy among the twelve selected compounds and a known ligand dataset (Oseltamivir, Zanamivir, Laninamivir, Peramivir).

(Fig. **7**) collectively shows binding mode of these screened compounds with binding site of H5N1 strain's Neuraminidase. It clearly shows that all ligands exhibit binding with critical binding residues of the receptor protein.

The detailed binding mode of these selected compounds from natural library of Princeton Database is shown in (Fig. **8**).

(Fig. **8**) clearly shows that the docked complexes of 12 compounds showed interactions with critical binding residues of the receptor. The residues involved in making interactions between the receptor protein and the 12 compounds along with details of their interaction modes are represented in Table **6**.

Docking results have demonstrated that natural compounds screened from the natural library of Princeton database may play an important role if validated by wet lab experiments for the inhibition of influenza virus. These newly reported ligands have same mode of interaction as that of known inhibitors of influenza virus. Hence, computational results have shown that these novel ligands may have the potential to inhibit influenza virus.

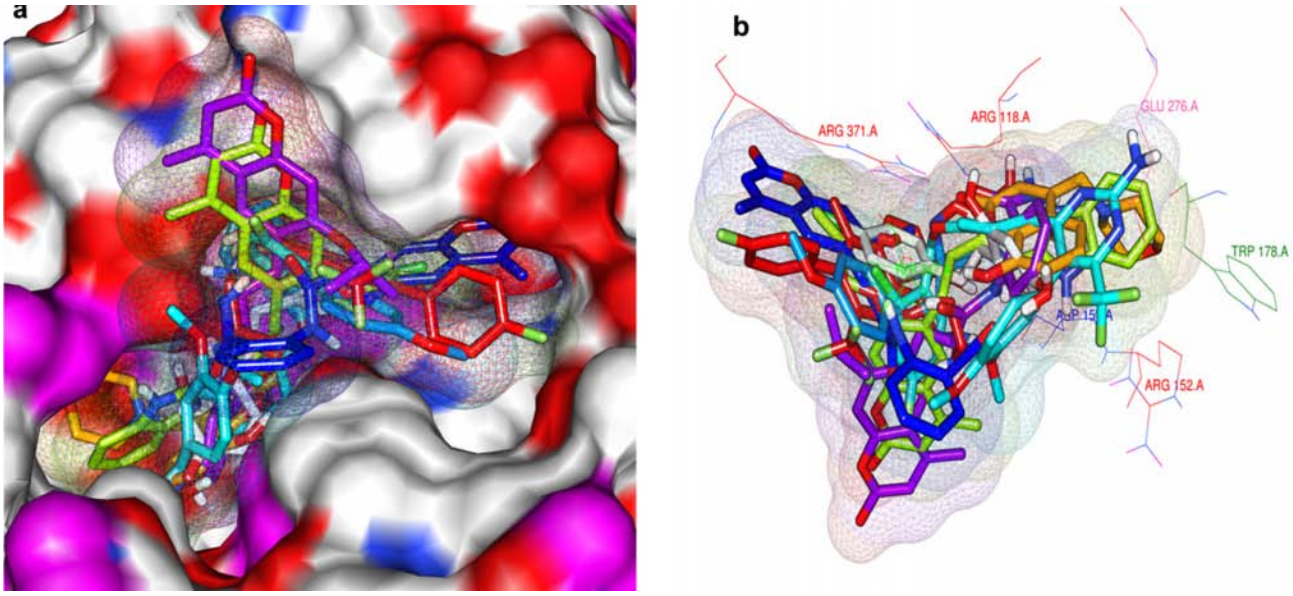

Fig. (7). Binding mode of screened compounds from Princeton Database with Neuraminidase (a) Ligands are shown as sticks in mesh surface and receptor as solid surface, (b) Ligands are shown as sticks surfaced by mesh while receptor residues are shown in lines and labeled.

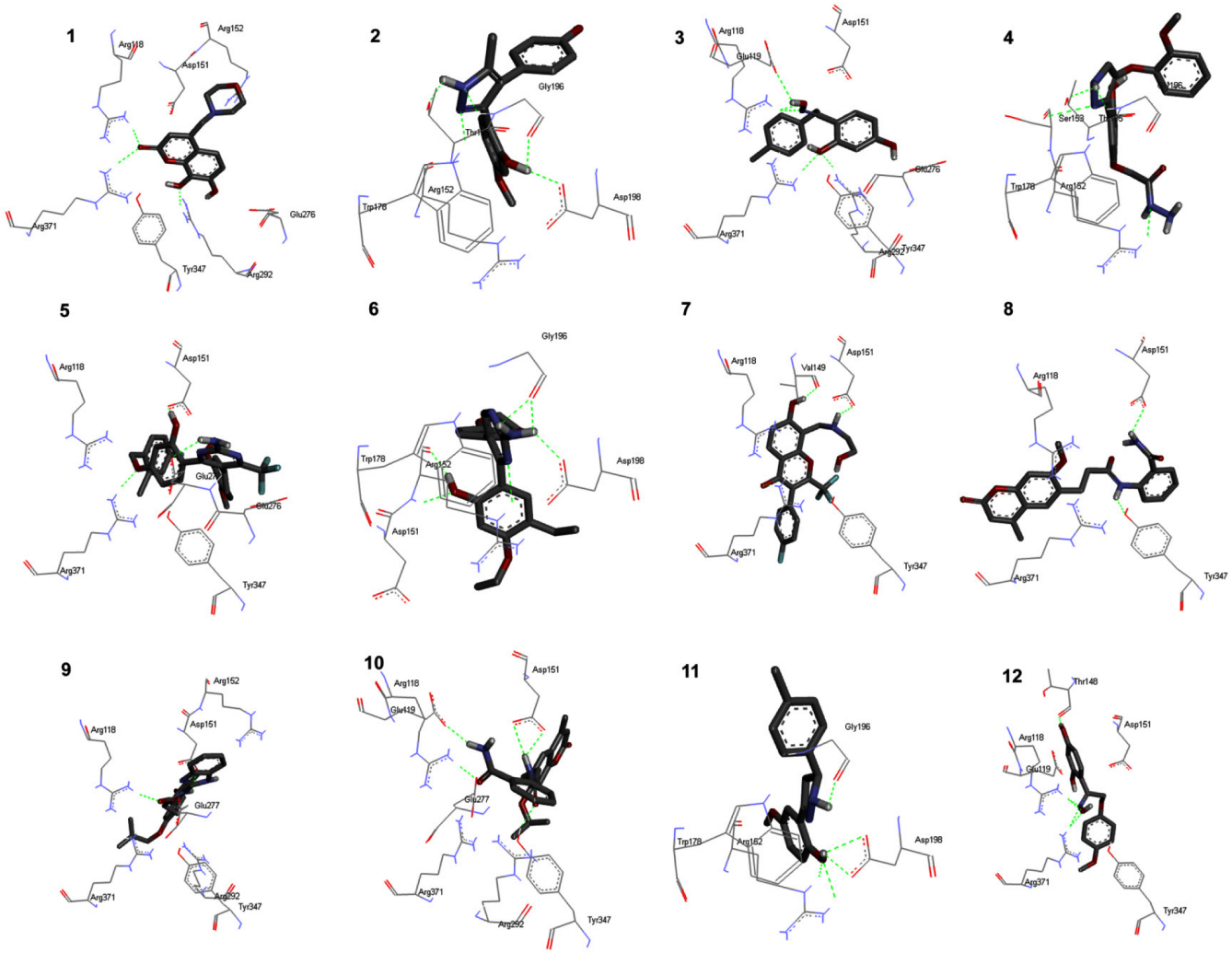

Fig. (8). Binding mode of screened 12 compounds with receptor H5N1, Hydrogen bonds are shown with green dotted lines. (For interpretation of the references to color in this figure legend, the reader is referred to the web version of this paper).

Table 6. Detailed binding interactions during docking of neuraminidase with the inhibitor data set. H represents a hydrogen bonding residue and HDP represents involvement of the residue in a hydrophobic interaction.

Residues	Arg118	Asp151	Arg152	Trp178	Glu276	Tyr347	Arg371
1	H	HDP	HDP	-	HDP	HDP	H
2	-	-	HDP	HDP	-	-	-
3	H	HDP	-	-	HDP	HDP	H
4	-	-	H	HDP	-	-	-
5	HDP	H	-	-	HDP	HDP	H
6	-	HDP	H	HDP	-	-	-
7	HDP	H	-	-	-	HDP	H
8	HDP	H	-	-	-	H	HDP
9	H	H	HDP	-	-	HDP	HDP
10	H	H	-	-	-	H	HDP
11	-	-	H	HDP	-	-	-
12	H	HDP	-	-	-	HDP	H

CONCLUSION

Theoretically, the neuraminidase inhibitors can effectively inhibit the activity of all neuraminidase subtypes, and therefore, they can be considered as candidates for the therapy of all strains of influenza [58]. In this study, we have used four neuraminidase inhibitors against H5N1 influenza virus strain. Computational studies were performed to check binding mode of these inhibitors against H5N1. Binding analysis showed that the four inhibitors bind well to the binding site of H5N1 strain. A ligand-based pharmacophore model was developed using this ligand dataset. Pharmacophoric features were identified which included one positive ionizable area, five hydrogen acceptors and three hydrogen donors. This pharmacophore model was used for the virtual screening of a library from Princeton Database. Compounds were screened from this library using different parameters. In the end, those compounds that showed pharmacophore features and bindings with H5N1 strain were reported. New ligands explored in the current study may have the prospective scope for managing the influence of influenza contagion, and are therefore suggested to be explored further for *in vivo* testing.

CONFLICT OF INTEREST

The authors confirm that this article content has no conflict of interest.

ACKNOWLEDGEMENTS

We are thankful to Comsats Institute of Information Technology, Islamabad for providing computational platform for carrying out the experiments.

LIST OF ABBREVIATIONS

2D = 2 Dimensional

3D = 3 Dimensional

VS = Virtual screening

HBA = Hydrogen bond acceptor

HBD = Hydrogen bond donor

PI = Positive ionizable area

HDP = Hydrophobic

REFERENCES

[1] Xu, X.; Zhu, X.; Dwek, R.A.; Stevens, J.; Wilson, I.A. Structural characterization of the 1918 influenza virus H1N1 neuraminidase. *J. Virol.*, **2008**, *82*, 10493-501.

[2] Russell, R.J.; Haire, L.F.; Stevens, D.J.; Collins, P.J.; Lin, Y.P.; Blackburn, G.M.; Hay, A.J.; Gamblin, S.J.; Skehel, J.J. The structure of H5N1 avian influenza neuraminidase suggests new opportunities for drug design. *Nature*, **2006**, *443*, 45-9.

[3] Bender, C.; Hall, H.; Huang, J.; Klimov, A.; Cox, N.; Hay, A.; Gregory, V.; Cameron, K.; Lim, W.; Subbarao, K. Characterization of the surface proteins of influenza A (H5N1) viruses isolated from humans in 1997-1998. *Virology*, **1999**, *254*, 115-23.

[4] Li, K.S.; Guan, Y.; Wang, J.; Smith, G.J.; Xu, K.M.; Duan, L.; Rahardjo, A.P.; Puthavathana, P.; Buranathai, C.; Nguyen, T.D. Genesis of a highly pathogenic and potentially pandemic H5N1 influenza virus in eastern Asia. *Nature*, **2004**, *430*, 209-13.

[5] Thompson, J.D.; Higgins, D.G.; Gibson, T.J. Improved sensitivity of profile searches through the use of sequence weights and gap excision. *Comput. Appl. Biosci.*, **1994**, *10*, 19-29.

[6] Varghese, J.N.; Laver, W.G.; Colman, P.M.. Structure of the influenza virus glycoprotein antigen neuraminidase at 2.9 A resolution. *Nature*, **1983**, *303*, 35-40.

[7] Baker, A.T.; Varghese, J.N.; Laver, W.G.; Air, G.M.; Colman, P.M. Three-dimensional structure of neuraminidase of subtype N9 from an avian influenza virus. *Proteins*, **1987**, *2*, 111-7.

[8] Ward, P.; Small, I.; Smith, J.; Suter, P.; Dutkowski, R. Oseltamivir (Tamiflu) and its potential for use in the event of an influenza pandemic. *J. Antimicrob. Chemother.*, **2005**, *55* (Suppl 1), i5-i21.

[9] Le, Q.M.; Kiso, M.; Someya, K.; Sakai, Y.T.; Nguyen, T.H.; Nguyen, K.H.; Pham, N.D.; Ngyen, H.H.; Yamada, S.; Muramoto, Y. Avian flu: isolation of drug-resistant H5N1 virus. *Nature*, **2005**, *437*, 1108.

[10] Kiso, M.; Mitamura, K.; Sakai-Tagawa, Y.; Shiraishi, K.; Kawakami, C.; Kimura, K.; Hayden, F.G.; Sugaya, N.; Kawaoka, Y. Re-

sistant influenza A viruses in children treated with oseltamivir: descriptive study. *Lancet*, **2004**, *364*,759-65.

[11] de Jong, M.D.; Tran, T.T.; Truong, H.K.; Vo, M.H.; Smith, G.J.; Nguyen, V.C.; Bach, V.C.; Phan, T.Q.; Do, Q.H.; Guan, Y. Oseltamivir resistance during treatment of influenza A (H5N1) infection. *N. Engl. J. Med*., **2005**, *353*, 2667-72.

[12] Karthick, V.; Ramanathan, K.; Shanthi, V.; Rajasekaran, R. Identification of potential inhibitors of H5N1 influenza A virus neuraminidase by ligand-based virtual screening approach. *Cell Biochem. Biophys*., **2013**, *66*, 657-69.

[13] Gong, K.; Li, L.; Wang, J.F.; Cheng, F.; Wei, D.Q.; Chou, K.C. Binding mechanism of H5N1 influenza virus neuraminidase with ligands and its implication for drug design. *Med. Chem*., **2009**, *3*, 242-9.

[14] Karthick, V.; Ramanathan, K. Virtual screening for oseltamivir-resistant a (H5N1) influenza neuraminidase from traditional Chinese medicine database: a combined molecular docking with molecular dynamics approach. *Springerplus*, **2013**, *2*, 115.

[15] Karthick, V.; Ramanathan, K. Insight into the oseltamivir resistance R292K mutation in H5N1 influenza virus: a molecular docking and molecular dynamics approach. *Cell Biochem. Biophys*., **2014**, *68*, 291-299.

[16] Schnell, J.R.; Chou, J.J. Structure and mechanism of the M2 proton channel of influenza A virus. *Nature*, **2008**, *451*, 591-595.

[17] Wang, J.; Pielak, R.M.; McClintock, M.A. Solution structure and functional analysis of the influenza B proton channel. *Nat. Struct. Mol. Biol*., **2009**, *16*, 1267-1271.

[18] Pielak, R.M.; Jason R. Schnell, J.R.; Chou, J.J. Mechanism of drug inhibition and drug resistance of influenza A M2 channel. *Proc. Natl. Acad. Sci. USA*, **2009**, *106*, 7379-7384.

[19] Call, M.E.; Chou, J.J. A view into the blind spot: solution NMR provides new insights into signal transduction across the lipid bilayer. *Structure*, **2010**, *18*, 1559-1569.

[20] Wang, S.Q.; Du, Q.S. Study of drug resistance of chicken influenza A virus (H5N1) from homology-modeled 3D structures of neuraminidases. *Biochem. Biophys. Res. Comm., (BBRC)*, **2007**, *354*, 634-640.

[21] Wang, S.Q.; Du, Q.S.; Huang, R.B. Insights from investigating the interaction of oseltamivir (Tamiflu) with neuraminidase of the 2009 H1N1 swine flu virus. *Biochem. Biophys. Res. Communications., (BBRC)*, **2009**, *386*, 432-436.

[22] Wang, J.F.; Wei, D.Q. Insights from investigating the interactions of adamantane-based drugs with the M2 proton channel from the H1N1 swine virus. *Biochem. Biophys. Res. Communications (BBRC)*, **2009**, *388*, 413-417.

[23] Du, Q.S.; Huang, R.B.; Wang, C.H. Energetic analysis of the two controversial drug binding sites of the M2 proton channel in influenza A virus. *J. Theor. Biol*., **2009**, *259*, 159-164.

[24] Wei, H.; Wang, C.H.; Du, Q.S. Investigation into adamantane-based M2 inhibitors with FB-QSAR. *Med. Chem*., **2009**, *5*, 305-317.

[25] Gong, K.; Li, L.; Wang, J.F. Binding mechanism of H5N1 influenza virus neuraminidase with ligands and its implication for drug design. *Med. Chem*., **2009**, *5*, 242-249.

[26] Du, Q.S.; Huang, R.B.; Wang, S.Q. Designing inhibitors of M2 proton channel against H1N1 swine influenza virus. *PLoS One*, **2010**, *5*, e9388.

[27] Wang, J.F. Insights from studying the mutation-induced allostery in the M2 proton channel by molecular dynamics. *Protein Eng. Des. Sel., (PEDS)*, **2010**, *23*, 663-666.

[28] Wang, S.Q.; Cheng, X.C.; Dong, W.L. Three new powerful Oseltamivir derivatives for inhibiting the neuraminidase of influenza virus. *Biochem. Biophys. Res. Commun., (BBRC)*, **2010**, *401*, 188-191.

[29] Li, X.B.; Wang, S.Q.; Xu, W.R. Novel inhibitor design for hemagglutinin against H1N1 influenza virus by core hopping method. *PLoS One*, **2011**, *6*, e28111.

[30] Berardi, M.J.; Shih, W.M.; Harrison, S.C. Mitochondrial uncoupling protein 2 structure determined by NMR molecular fragment searching. *Nature*, **2011**, *476*, 109-113.

[31] OuYang, B.; Xie, S.; Berardi, M.J. Unusual architecture of the p7 channel from hepatitis C virus. *Nature*, **2013**, *498*, 521-525.

[32] Call, M.E.; Schnell, J.R.; Xu, C. The structure of the zetazeta transmembrane dimer reveals features essential for its assembly with the T cell receptor. *Cell*, **2006**, *127*, 355-368.

[33] Call, M.E.; Wucherpfennig, K.W.; Chou, J.J. The structural basis for intramembrane assembly of an activating immunoreceptor complex. *Nat. Immunol*., **2010**, *11*, 1023-1029.

[34] Jones, D.; Heinrikson, R.L. Prediction of the tertiary structure and substrate binding site of caspase-8. *FEBS Lett*., **1997**, *419*, 49-54.

[35] Tomasselli, A.G.; Heinrikson, R.L. Prediction of the Tertiary Structure of a Caspase-9/Inhibitor Complex. *FEBS Lett*., **2000**, *470*, 249-256.

[36] Wang, J.F.; Wei, D.Q.; Li, L. 3D structure modeling of cytochrome P450 2C19 and its implication for personalized drug design. *Biochem Biophys Res Commun (BBRC) (Corrigendum: ibid*, 2007, Vol. *357*, 330), **2007**, *355*, 513-519.

[37] Chou, K.C. Coupling interaction between thromboxane A2 receptor and alpha-13 subunit of guanine nucleotide-binding protein. *J. Proteome Res*., **2005**, *4*, 1681-1686.

[38] Chou, K.C. Review: Structural bioinformatics and its impact to biomedical science. *Curr. Med. Chem*., **2004**, *11*, 2105-2134.

[39] Gubareva, L.V. Molecular mechanisms of influenza virus resistance to neuraminidase inhibitors. *Virus. Res*., **2004**, *103*, 199-203.

[40] Russell, R.J.; Haire, L.F.; Stevens, D.J.; Collins, P.J.; Lin, Y.P.; Blackburn, G.M.; Hay, A.J.; Gamblin, S.J.; Skehel, J.J. The structure of H5N1 avian influenza neuraminidase suggests new opportunities for drug design. *Nature* **2006**, *443*, 45-9.

[41] Watenpaugh, K.D.; Heinrikson, R.L. A Model of the complex between cyclin-dependent kinase 5 (Cdk5) and the activation domain of neuronal Cdk5 activator. *Biochem. Biophys. Res. Communications., (BBRC)*, **1999**, *259*, 420-428.

[42] Zhang, J.; Luan, C.H. Identification of the N-terminal functional domains of Cdk5 by molecular truncation and computer modeling. *Proteins: Struct., Funct., Genet*., **2002**, *48*, 447-453.

[43] Wei, D.Q.; Zhong, W.Z. Binding mechanism of coronavirus main proteinase with ligands and its implication to drug design against SARS. (Erratum: ibid., 2003, Vol. 310, 675). *Biochem. Biophys. Res. Comm. (BBRC)*, **2003**, *308*, 148-151.

[44] Huang, R.B.; Du, Q.S.; Wang, C.H. An in-depth analysis of the biological functional studies based on the NMR M2 channel structure of influenza A virus. *Biochem. Biophys. Res. Comm. (BBRC)*, **2008**, *377*, 1243-1247.

[45] Chou, K.C. Molecular therapeutic target for type-2 diabetes. *J. Proteome Res*., **2004**, *3*, 1284-1288.

[46] Wang, J.F. Insights from modeling the 3D structure of New Delhi metallo-beta-lactamase and its binding interactions with antibiotic drugs. *PLoS One*, **2011**, *6*, e18414.

[47] Wang, J.F. Insights into the Mutation-Induced HHH syndrome from modeling human mitochondrial ornithine transporter-1. *PLoS One*, **2012**, *7*, e31048.

[48] Morris, G.M.; Goodsell, D.S.; Halliday, R.S.; Huey, R.; Hart, W. E.; Belew, R.K.; Olson, A.J. Automated docking using a lamarckian genetic algorithm and and empirical binding free energy function. *J. Comp. Chem*., **1998**, *19*, 1639-1662.

[49] Wang, J.F. Insight into the molecular switch mechanism of human Rab5a from molecular dynamics simulations. *Biochem. Biophys. Res. Commun. (BBRC)*, **2009**, *390*, 608-612.

[50] Wang, J.F.; Gong, K.; Wei, D.Q. Molecular dynamics studies on the interactions of PTP1B with inhibitors: from the first phosphate-binding site to the second one. *Protein Eng. Des. Sel., (PEDS)*, **2009**, *22*, 349-355.

[51] Chou, K.C. Low-frequency resonance and cooperativity of hemoglobin. *Trends Biochem. Sci*., **1989**, *14*, 212-213.

[52] Mao, B. Collective motion in DNA and its role in drug intercalation. *Biopolymers*, **1988**, *27*, 1795-1815.

[53] Chou, K.C. Review: Low-frequency collective motion in biomacromolecules and its biological functions. *Biophys. Chem*., **1988**, *30*, 3-48.

[54] Wolber, G.; Langer, T. LigandScout: 3-D pharmacophores derived from protein-bound ligands and their use as virtual screening filters. *J. Chem. Inf. Model*., **2005**, *45*, 160-9.

[55] Sirois, S.; Wei, D.Q.; Du, Q.S. Virtual Screening for SARS-CoV Protease Based on KZ7088 Pharmacophore Points. *J. Chem. Inf. Comput. Sci*., **2004**, *44*, 1111-1122.

[56] Wei, D.Q.; Du, Q.S. Review: Progress in computational approach to drug development against SARS. *Curr. Med. Chem*., **2006**, *13*, 3263-3270.

[57] Zhang, T.; Wei, D.Q. A pharmacophore model specific to active site of CYP1A2 with a novel molecular modeling explorer and CoMFA. *Med. Chem*., **2012**, *8*, 198-207.

[58] Sultana, I.; Gao, J.; Markoff, L.; Eichelberger, M.C. Influenza neuraminidase-inhibiting antibodies are induced in the presence of zanamivir. *Vaccine*, **2011**, *29*, 2601-6.

Received: January 25, 2015 Revised: June 29, 2015 Accepted: July 03, 2015